Characteristics and Evaporation History of Fuel Spray Injected into Crossflowing Airstreams

Jun Yong Zhu*
Beijing Institute of Aeronautics and Astronautics, Beijing, China
and
Ju Shan Chin†
Purdue University, West Lafayette, Indiana

A numerical calculation method is used to predict the variation in the characteristics of a fuel spray injected into high-temperature crossflowing airstreams, namely, the variation in Sauter mean diameter, droplet size distribution parameter N of the Rosin-Rammler distribution, and evaporation percentage of the spray Q_{EV} with downstream distance X from the nozzle. The effects of the droplet heating period and forced convection on the evaporation process have been taken into account; thus, the calculation model is a good approximation to the process of spray evaporation in practical combustors, such as afterburner, ramjet, etc. The variations in the spray characteristics and evaporation percentage Q_{EV} with the downstream distance for different air velocities, pressures, temperatures, fuel injection velocities, and initial spray conditions are presented.

Nomenclature

A,B	= constants in Eq. (8)
B_y	= mass transfer number
C_D	= droplet drag coefficient
C_{EX}	= thermal expansion coefficient of liquid fuel
C_F	= specific heat of liquid fuel
C_P	= specific heat of gas
D	= droplet diameter
$\bar{D}$	= mean diameter in a droplet size increment
ΔD	= droplet size increment
h	= convective heat-transfer coefficient
K	= thermal conductivity
L	= latent heat of fuel
M	= molecular mass
$\dot{M}_F$	= rate of droplet evaporation
MMD	= mass median diameter
N	= droplet size distribution parameter in Rosin-Rammler distribution
p	= pressure
Pr	= Prandtl number
Q	= volume fraction contained in droplets of diameter less than D
Q_e, Q_Σ	= heat used for fuel evaporation, heat transferred from air
Q_{EV}	= evaporation percentage of fuel spray
r_s	= droplet radius
Sc	= Schmidt number
Sh	= Sherwood number
T	= temperature
t	= time
Δt	= time increment
$\bar{U}, U_x, U_y$	= relative velocity of droplets
$\bar{V}, V_x, V_y$	= true velocity of droplets
Y	= gaseous mass fraction
ρ	= density
μ	= viscosity

Subscripts

A	= air
BN	= normal boiling
CR	= critical
F	= liquid fuel or fuel vapor
G	= gas
R	= reference
s	= droplet surface
0	= initial
∞	= far upstream
Σ	= surrounding

Received March 7, 1986; presented as Paper 86-1528 at the AIAA/SAE/ASME/ASEE 22nd Joint Propulsion Conference, Huntsville, AL, June 16-18, 1986; revision received July 24, 1986.
Copyright © American Institute of Aeronautics and Astronautics, Inc., 1987. All rights reserved.

*Graduate Student.
†Visiting Professor of Mechanical Engineering.

Introduction

SPRAY combustion has become a very attractive and important branch of combustion science in recent years, involving heat and mass transfer, chemical reaction, turbulence, two-phase flow, and other very interesting aspects. So far, research on liquid-fuel atomization and evaporation has been very active. But the diagnostic technique for fuel spray combustion has not been developed to the point that the characteristics of a burning spray can be determined with confidence. The understanding of the variations in spray characteristics under pure evaporation (without combustion) will help combustion engineers to understand the fuel spray/air mixture formation in combustors such as afterburners.

A lot of research work has been done on the spray characteristics of injector atomization and on droplet and spray evaporation. However, little has been published on systematic studies of the interdependence between fuel spray characteristics and spray evaporation history, by which we mean the influence of different fuel spray characteristics on the spray evaporation rate and the influence of spray evaporation history on spray characteristics. Some preliminary work has been reported in a previous paper[1] in which it was shown that the droplet size distribution parameter N in the Rosin-Rammler distribution has an important influence on spray evaporation history. A larger value of N has a lower 90% evaporation time, but a higher 20% evaporation time, which means that a larger value of N is beneficial for combustion efficiency but provides less initial evaporation for ignition. It was also shown that for N values less than 4, which are the practical situation for most sprays formed by atomizers, the mass median diameter (MMD) and the droplet size distribution parameter will both increase with evaporation history.

But the results obtained in Ref. 1 were for "stagnant" sprays, which are obviously unpractical. The incentive for the present work was to expand the scope of the study from a stagnant spray to a moving spray in an airstream to see whether these conclusions were still valid. The variations in fuel spray characteristics and spray evaporation fraction at different positions downstream of an injector in cross-flowing, high-temperature airstreams are reported. (See Fig. 1.)

Analysis of Evaporation Process in a Moving Droplet

Heat-Transfer Analysis

The heat transferred to a droplet moving in a hot airflow can be expressed as

$$Q_\Sigma = 4\pi r_s^2 h (T_\infty - T_s) \tag{1}$$

The heat-transfer coefficient equation for a droplet under steady-state evaporation can be written as

$$Nu = \frac{2 \cdot h \cdot r_s}{K_G} = 2 \cdot \frac{\ell n(1+B_y)}{B_y} \tag{2}$$

Ranz and Marshall[2] gave an empirical correlation that is generally used to account for the effect of forced convection. Based on this correlation, the enhancement of heat transfer by forced convection can be expressed as

$$h/h_{Re=0} = 1 + 0.3 Re^{1/2} Pr^{1/3} \tag{3}$$

More recently, Faeth[3] proposed a multiplicative correction for convection as

$$\frac{h}{h_{Re=0}} = 1 + \frac{0.277 \cdot Re^{1/2} Pr^{1/3}}{[1 + (1.232/Re \cdot Pr^{4/3})]^{1/2}} \tag{4}$$

But within the range of Reynolds number encountered in the present study, the difference between Eqs. (3) and (4) is rather small, so Eq. (3) will be used later. Thus, the heat-transfer coefficient for a vaporizing droplet with forced convection is written as

$$h = \frac{K_G}{r_s}(1 + 0.3 Re^{1/2} Pr^{1/3}) \cdot \frac{\ell n(1+B_y)}{B_y} \tag{5}$$

For numerical calculation, B_y is defined as the mass transfer number by

$$B_y = Y_{Fs}/(1 - Y_{Fs}) \tag{6}$$

and Y_{Fs} is the fuel vapor mass fraction at the droplet surface, which can be calculated by[4]

$$Y_{Fs} = \left[1 + \left(\frac{P_\Sigma}{P_{Fs}} - 1\right)\frac{M_A}{M_F}\right]^{-1} \tag{7}$$

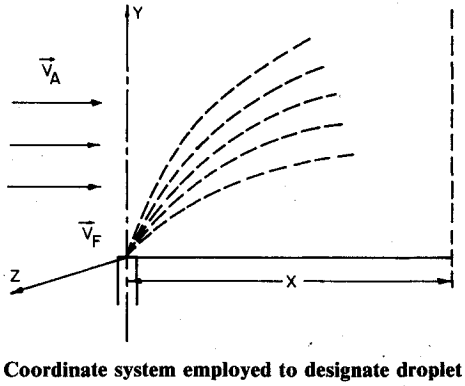

Fig. 1 Coordinate system employed to designate droplet motion.

while P_{Fs} is the partial pressure of the fuel vapor at the droplet surface and can be calculated by a modified Clausius-Clapeyron equation proposed in Ref. 4,

$$P_{Fs} = \exp\left(A - \frac{B}{T_s - 43}\right) \tag{8}$$

Thus, the heat transferred from the hot air to a moving, vaporizing droplet is

$$Q_\Sigma = 4\pi r_s K_G (T_\infty - T_s)(1 + 0.3 Re^{1/2} Pr^{1/3}) \cdot \frac{\ell n(1+B_y)}{B_y} \tag{9}$$

Heat Used for Droplet Evaporation

Latent heat consumed for droplet evaporation is

$$Q_e = \dot{M}_F \cdot L \tag{10}$$

For a spherical droplet Spalding[5] proposed an expression for the prediction of evaporation rate of a stagnant droplet as

$$\dot{M}_F = 4\pi r_s \frac{K_G}{C_{pG}} \ell n(1+B_y) \tag{11}$$

If the forced convection is taken into account,[2] then

$$(Sh/Sh_{Re=0}) = 1 + 0.3 Re^{1/2} Pr^{1/3} \tag{12}$$

Assuming the Lewis number is unity, we have

$$\dot{M}_F = 4\pi r_s \frac{K_G}{C_{pG}}(1 + 0.3 \cdot Re^{1/2} Pr^{1/3}) \ell n(1+B_y) \tag{13}$$

while the latent heat of fuel can be expressed as[6]

$$L = L_{T_{BN}} \left(\frac{T_{CR} - T_s}{T_{CR} - T_{BN}}\right)^{0.38} \tag{14}$$

Thus we have

$$Q_e = 4\pi r_s \frac{K_G}{C_{pG}}(1 + 0.3 Re^{1/2} Pr^{1/3}) \ell n(1+B_y) \cdot L_{T_{BN}} \left(\frac{T_{CR} - T_s}{T_{CR} - T_{BN}}\right)^{0.38} \tag{15}$$

Analysis of Evaporation Process

The evaporation process of a fuel droplet can be described as follows: at beginning, the heat transferred from hot air to the fuel droplet is partially used for heating the droplet and

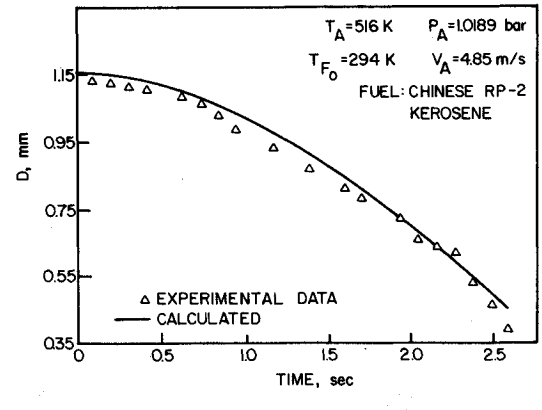

Fig. 2 Comparison between calculated liquid-fuel droplet evaporation history and experimental data.

partially consumed for the evaporation latent heat. Later, as the temperature of droplet rises and the evaporation rate increases, more heat is used for latent heat and less for heating the droplet, until the droplet temperature reaches the so-called wet bulb temperature. After this point, all of the heat transferred from the hot air will be used as the latent heat of evaporation and the droplet temperature will remain constant. Assuming the existence of a strong recirculation inside the droplet, that is, neglecting the temperature gradient within the droplet, we may write the energy equation for a droplet as

$$Q_\Sigma - Q_e = \frac{4}{3} \cdot \pi \cdot r_s^3 \cdot \rho_F \cdot C_F \cdot \frac{dT_s}{dt} \tag{16}$$

or

$$\frac{dT_s}{dt} = \frac{3}{4\pi r_s^3} \cdot \frac{Q_\Sigma - Q_e}{\rho_F \cdot C_F} \tag{17}$$

Within each time increment Δt, Eq. (13) is still valid and

$$\dot{M}_F = -\frac{d}{dt}\left(\frac{4}{3}\pi r_s^3 \cdot \rho_F\right) \tag{18}$$

Combining Eqs. (13) and (18), we have

$$\frac{dr_s}{dt} = -\frac{K_G}{C_{P_G}\rho_F r_s} \ln(1+B_y)(1+0.3Re^{1/2}Pr^{1/3}) \tag{19}$$

Equations (17) and (19) are essential for the prediction to be carried out in this paper. Thus, the authors conducted a separate experiment using a suspended droplet on a thermocouple wire and a cinema camera to take photos of the history of vaporizing droplet in heated airflow. The result obtained was compared with the prediction made by Eqs. (17) and (19), as shown in Fig. 2. It shows clearly that the agreement is very good.

Droplet Trajectory Equation

Droplet Drag Coefficient

Based on experience with liquid-fuel distribution and droplet trajectory experiments and calculations, the authors are sure that using the far upstream air density and one-third role of averaging proposed by Sparrow and Gregg[7] to determine the viscosity of fuel/vapor/air mixture, the "standard" form (without evaporation) of droplet drag coefficient can be used for the evaporizing droplet,

$$C_D = \frac{24}{Re}\left(1+\frac{1}{6}Re^{2/3}\right) \quad Re < 350$$

$$= 0.178 \cdot Re^{0.217} \quad Re > 350 \tag{20}$$

Droplet Motion Equation

Neglecting the gravity and buoyancy of the droplet, we may write the droplet motion equation as

$$\frac{1}{6} \cdot \rho_F \cdot \pi D^3 \frac{dU}{dt} = -C_D \cdot \left(\frac{1}{2}\rho_A U^2\right) \bar{i_U} \cdot \frac{1}{4}\pi D^2 \tag{21}$$

So

$$\frac{dU}{dt} = -\frac{3}{8}\frac{\rho_A}{\rho_F}\frac{U^2}{r_s} C_D \bar{i_U} \tag{22}$$

By solving Eqs. (17), (19), and (22) simultaneously using Runge-Kutta numerical method, the droplet temperature T_s, radius r_s, and relative velocity U can be obtained. Then, we have

$$\bar{V}_D = \bar{V}_a + \bar{U} \tag{23}$$

and

$$X = \int_0^t V_{DX} dt = \int_0^t (V_{AX} + U_X) dt$$

$$y = \int_0^t V_{Dy} dt = \int_0^t (V_{Ay} + U_y) dt \tag{24}$$

Physical Properties

In order to carry out the calculation, the physical properties of the fuel, fuel vapor, and air must be known. These are so important that the results will be meaningless if the physical properties are not determined correctly. The properties of air can easily be found in related handbooks; thus, only the physical properties of fuel and fuel vapor will be mentioned here.

The fuel density is

$$\rho_F = \rho_{F0}\left[1 - 1.8C_{EX}(T_s - 288.6) - 0.09\frac{(T_s-288.6)^2}{(T_{CR}-288.6)^2}\right] \tag{25}$$

the specific heat of fuel vapor,

$$C_{P_F} = (0.363 + 0.00046T_R)(5 - 0.001\rho_{F0}) \tag{26}$$

the thermal conductivity of fuel vapor

$$K_F = [13.2 - 0.0313(T_{BN} - 273.16)] \cdot \left(\frac{T_R}{273.16}\right)^m \cdot 10^{-6} \tag{27}$$

where

$$m = 2.0 - 0.0372(T_R/T_{BN})^2 \tag{28}$$

and the viscosity of fuel vapor

$$\mu_F = [760 + 3.6(T_R - 400)] \cdot 10^{-8}$$

$$300 < T_R < 600 \tag{29a}$$

$$= [2120 + 1.8286(T_R - 950)] \times 10^{-8}$$

$$600 < T_R < 950 \tag{29b}$$

where T_R is the reference temperature, which is, according to the one-third rule of Sparrow and Gregg,[7]

$$T_R = T_s + \tfrac{1}{3}(T_\infty - T_s) = T_s + \tfrac{1}{3}(T_A - T_s) \tag{30}$$

The specific heat, thermal conductivity, and viscosity of fuel vapor/air mixture are

$$C_{P_G} = C_{P_A} \cdot Y_{AR} + C_{P_F} \cdot Y_{FR} \tag{31}$$

$$K_G = K_A Y_{AR} + K_F Y_{FR} \tag{32}$$

$$\mu_G = \mu_A Y_{AR} + \mu_F Y_{FR} \tag{33}$$

where

$$Y_{FR} = Y_{Fs} + \tfrac{1}{3}(Y_{F\infty} - Y_{Fs}) \tag{34}$$

assuming $Y_{F\infty} = 0$, we have

$$Y_{FR} = \tfrac{2}{3} Y_{Fs} \tag{35}$$

$$Y_{AR} = 1 - \tfrac{2}{3} Y_{Fs} \tag{36}$$

The normal boiling temperature T_{BN}, critical temperature T_{CR}, latent heat L_{TBN}, density ρ_{F0}, thermal conductivity K_{F0}, thermal expansion coefficient C_{EX}, molecular mass M_F, and the constants A and B in Eq. (8) for Chinese kerosine RP-2 are listed in Table 1.

Variation of Spray Characteristics with Evaporation Process

We assume that the initial droplet size distribution can be expressed by the Rosin-Rammler (R-R) distribution as

$$Q = 1 - \exp[-0.693(D/\mathrm{MMD})^N] \tag{37}$$

The calculation of the variation of spray characteristics with evaporation process is carried out according to the following steps:

1) For a given initial spray with given N and MMD values, we divide the spray into a series of dropsize increments with each size increment

$$\Delta D_i = 0.02\ \mathrm{MMD}$$

and the maximum droplet diameter is assumed to be

$$D_{\max} = 6.5(\mathrm{MMD}/N) \tag{38}$$

This empirical correlation has taken into consideration the effects of both parameter N and MMD in the R-R distribution on the determination of maximum diameter for calculation. The $Q_{D\max}$ corresponding to the $D_{\max}$ determined by Eq. (38) is extremely close to 100% (the difference is less than 10^{-6}). Also, this $D_{\max}$ value will not cause the calculation too much CPU time.

For each dropsize increment, $\bar{D}_i = \frac{1}{2}(D_i + D_{i+1})$ is taken as the representative diameter and the volume fraction increment is

$$\Delta Q_i = 0.693N\frac{\bar{D}_i^{N-1}}{\mathrm{MMD}^N}\cdot\exp\left[-0.693\left(\frac{\bar{D}_i}{\mathrm{MMD}}\right)^N\right]\Delta D_i \tag{39}$$

2) Assume a suitable axial distance increment, calculate the time required for each droplet group to pass this distance, $\Delta t_{ij} = \Delta X_j / V_{Dxi}$.

3) By solving Eqs. (17), (19), and (22) simultaneously, calculate the droplet size $\bar{D}_{ij}$ after each distance increment ΔX_j.

4) Calculate the fraction of liquid fuel remaining in each droplet group after the distance increment

$$\Delta X_j \quad \text{as} \quad \Delta Q_{ij} = \Delta Q_{ij-1}(\bar{D}_{ij}/\bar{D}_{ij-1})^3 \tag{40}$$

5) Thus, the total volume fraction of liquid fuel for the whole spray remaining after the distance increment ΔX_j is $Q_{ij} = \Sigma_i \Delta Q_{ij}$.

Table 1 Properties of Chinese kerosine RP-2

T_{BN}	457.65 K
T_{CR}	648.40 K
L_{TBN}	279.25 kJ/kg
K_{F0}	1.1888×10^{-4} kJ/ms·K
ρ_{F0}	776 kg/m^3
M_F	144.2
A	15.1962
B	4384.22
C_{EX}	5.21×10^{-4}

Table 2 Quantities used for calculations

$p = 1.05\times10^5$ Pa	$T_A = 500$ K
$V_{AX} = 51$ m/s	$V_{AY} = 0$ m/s
$T_{s0} = 313$ K	$V_F = 36.9$ m/s
$N = 2.5$	MMD = 50 μm

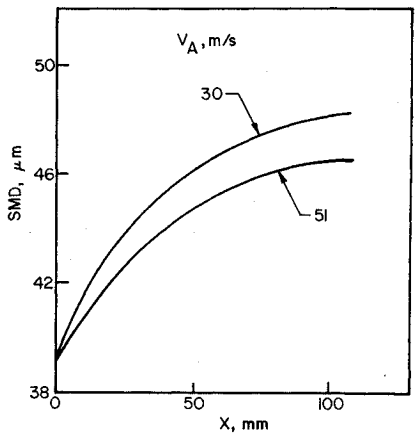

a) Effect of air velocity V_A on the change in SMD along the axial distance.

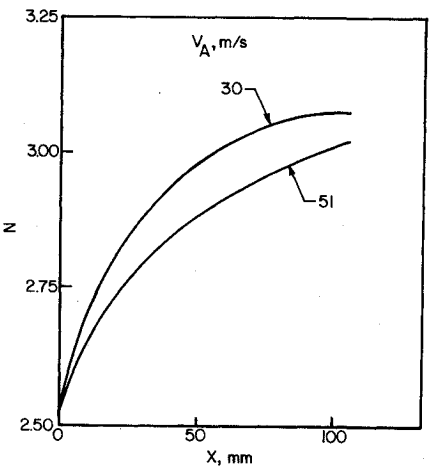

b) Effect of air velocity V_A on the change in spray size distribution parameter N along the axial distance.

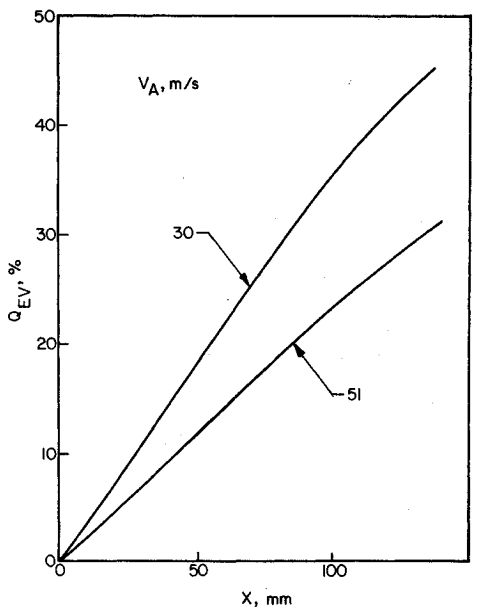

c) Effect of air velocity V_A on the change in spray evaporation percentage Q_{EV} along the axial distance.

Fig. 3 Effect of air velocity V_A.

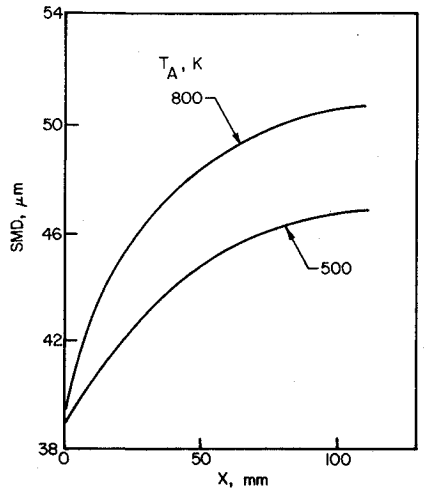

a) Effect of air temperature T_A on the change in SMD along the axial distance.

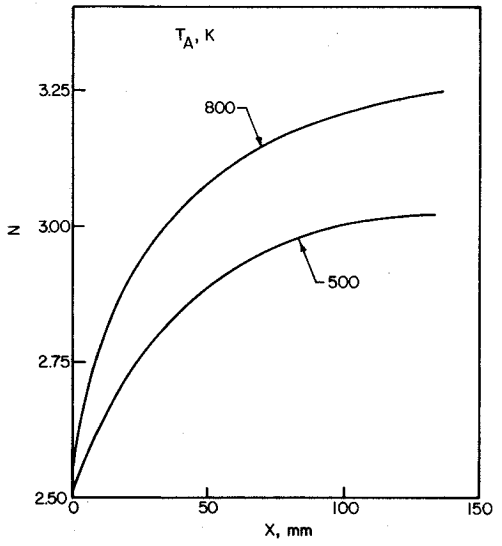

b) Effect of air velocity T_A on the change in spray size distribution parameter N along the axial distance.

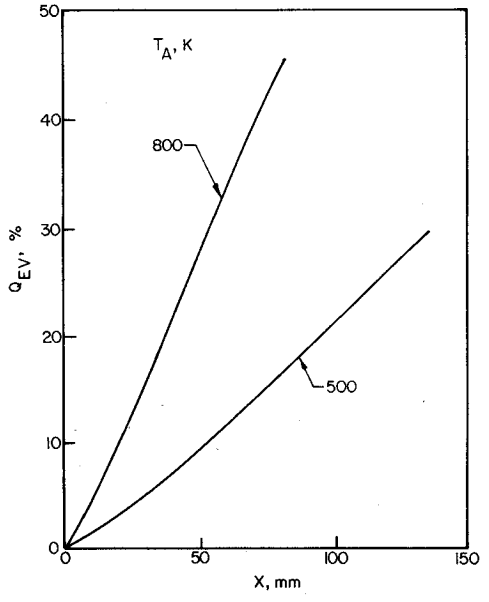

c) Effect of air velocity T_A on the change in spray evaporation percentage Q_{EV} along the axial distance.

Fig. 4 Effect of air temperature T_A.

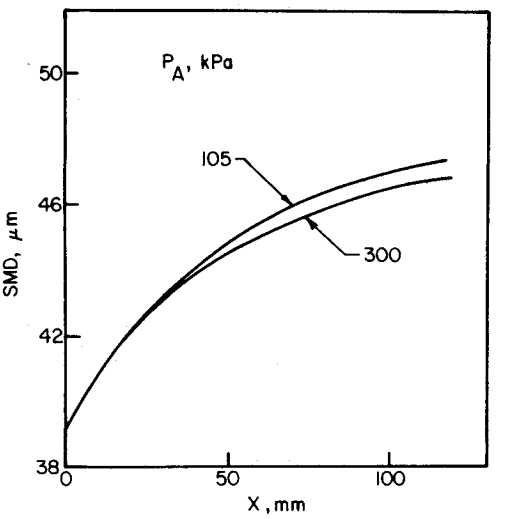

a) Effect of air pressure P_A on the change in SMD along the axial distance.

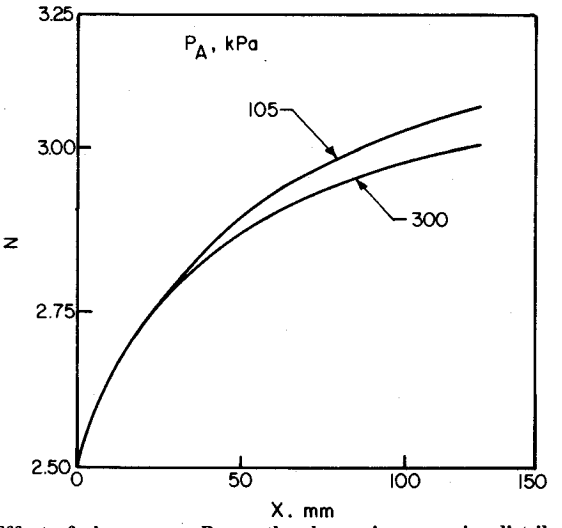

b) Effect of air pressure P_A on the change in spray size distribution parameter N along the axial distance.

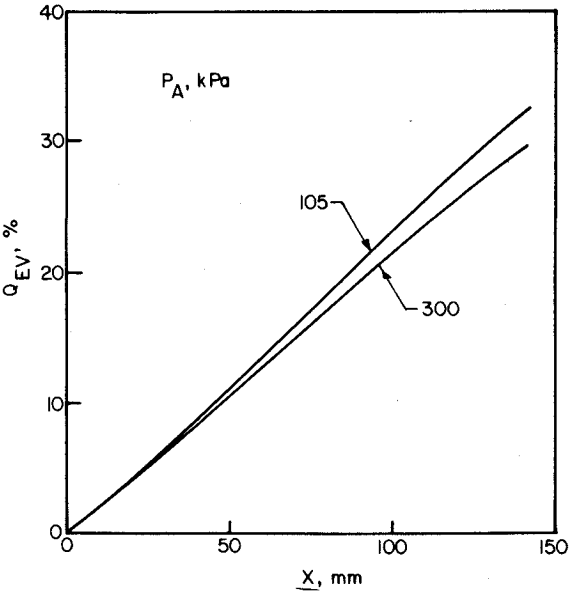

c) Effect of air pressure P_A on the change in spray evaporation percentage Q_{EV} along the axial distance.

Fig. 5 Effect of air pressure P_A.

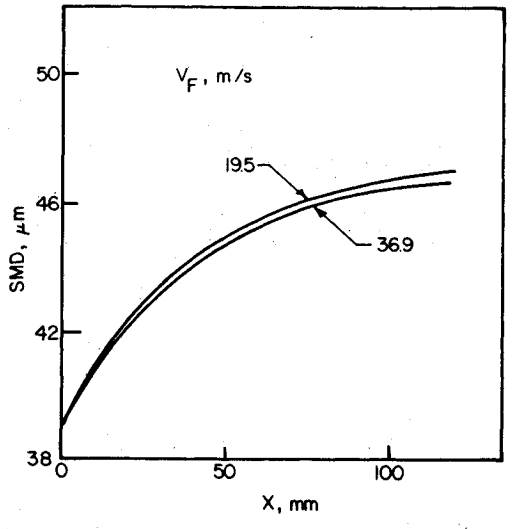

a) Effect of fuel injection velocity V_F on the change in SMD along the axial distance.

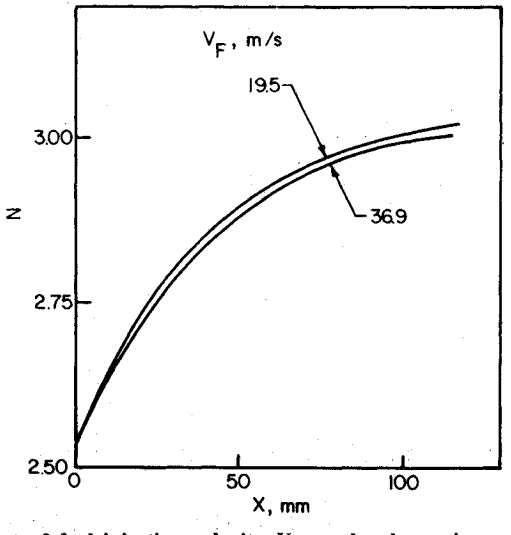

b) Effect of fuel injection velocity V_F on the change in spray size distribution parameter N along the axial distance

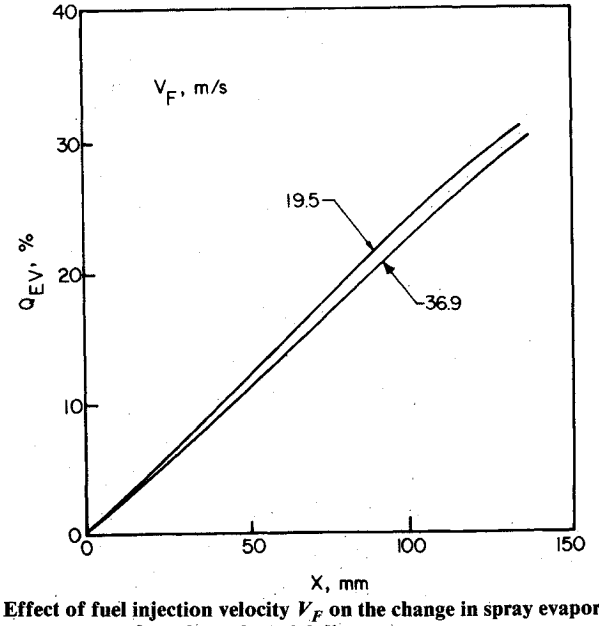

c) Effect of fuel injection velocity V_F on the change in spray evaporation percentage Q_{EV} along the axial distance.

Fig. 6 Effect of fuel injection velocity V_F.

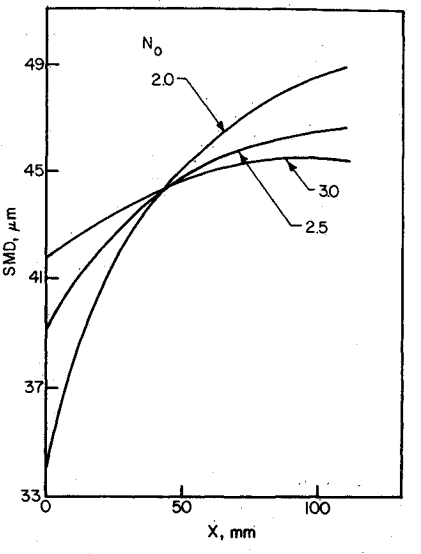

a) Effect of the initial value of N on the change in SMD along the axial distance.

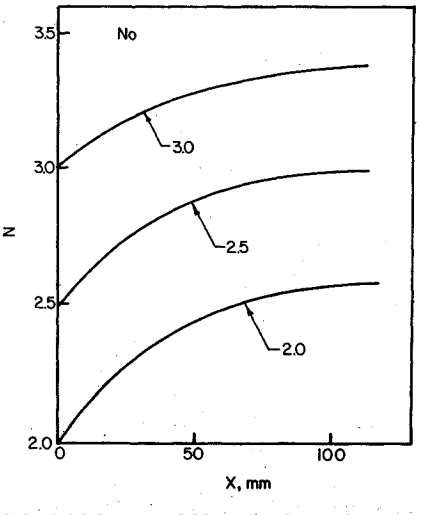

b) Effect of the initial value of N on the change in spray size distribution parameter N along the axial distance.

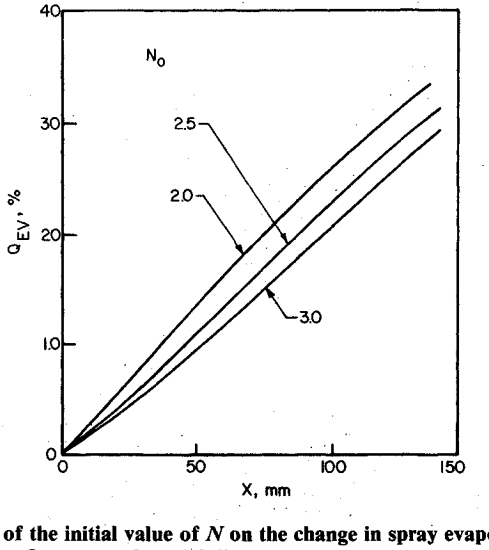

c) Effect of the initial value of N on the change in spray evaporation percentage Q_{EV} along the axial distance.

Fig. 7 Effect of the initial value of N.

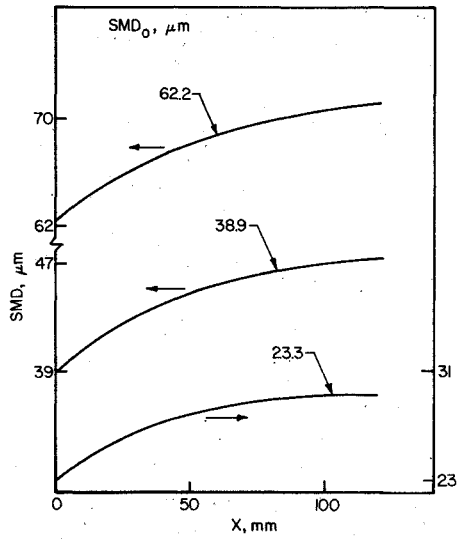

a) Effect of the initial value of SMD on the change in SMD along the axial distance.

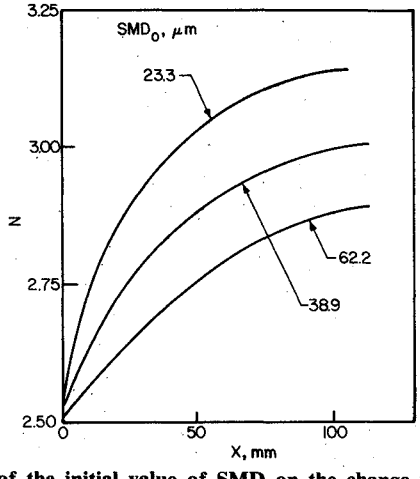

b) Effect of the initial value of SMD on the change in spray size distribution parameter N along the axial distance.

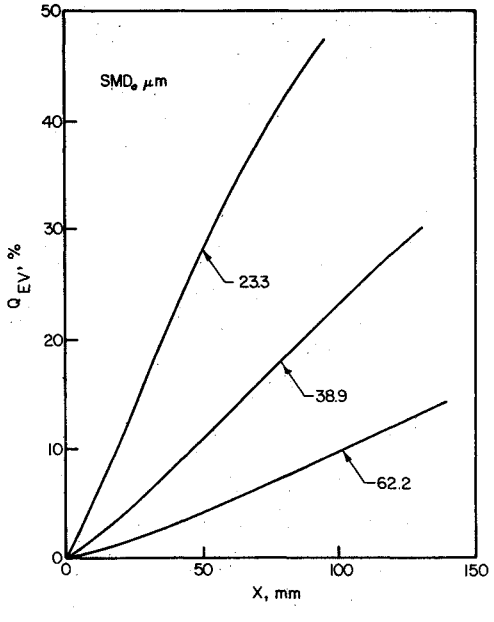

c) Effect of the initial value of SMD on the change in spray evaporation percentage Q_{EV} along the axial distance.

Fig. 8 Effect of the initial value of SMD.

6) Calculate the new droplet size distribution

$$\Delta Q'_{ij} = \Delta Q_{ij} / Q_{ij} \tag{41}$$

$$Q'_{ij} = \Sigma_i \Delta Q'_{ij} \tag{42}$$

7) The liquid fuel remaining in the spray at the end of X_j is

$$Q_{Tj} = Q_{Tj-1} \cdot \Sigma_i \Delta Q_{ij}$$

The quantity of fuel evaporized is

$$Q_{EV} = 1 - Q_{Tj} \tag{43}$$

8) Rewrite Eq. (37) as

$$\ell nD = \frac{1}{N} \cdot \ell n \left[\frac{\ell n(1-Q)^{-1}}{0.693} \right] + \ell n(\mathrm{MMD}) \tag{44}$$

using the least square method for ℓnD and $\ell n[\ell n(1-Q)^{-1}/0.693]$, the new spray characteristics MMD′ and N' can be determined; then, the new Sauter mean diameter can be obtained by

$$\mathrm{SMD}' = \left[\frac{N}{N-1} \Gamma\left(2 - \frac{1}{N}\right) \cdot (0.693)^{1/N} \right]^{-1} \cdot \mathrm{MMD} \tag{45}$$

9) For the next distance increment ΔX_{j+1}, repeat steps 2-7. Thus, the fuel spray characteristics MMD or SMD, N, and the quantity of fuel evaporated Q_{EV} as functions of downstream distance X can be determined.

Calculation Results

Typical quantities used for calculating the results are shown in Table 2.

The calculation results are shown in Figs. 3-8. They show clearly that the spray characteristics SMD, N, and the quantity of fuel evaporized Q_{EV} are increased with the downstream distance X. The variation of SMD with the downstream distance is rather sharp at the beginning, but then decreases. This is due to the fact that small droplets extinguish within a short distance from the nozzle. The same trend has been observed for N values.

As shown in Fig. 3, with the increase in air velocity, the evaporation percentage Q_{EV} lessens. Higher air velocities will enhance fuel droplet evaporation, but also allow shorter residence times for the droplets to reach certain downstream distances. Also, the variations in spray characteristics with downstream distance decrease.

With the increase of air temperature T_A, the evaporation percentage increases dramatically. Also, the variation in spray characteristics with downstream distance is more significant, as shown in Fig. 4.

Figure 5 shows that air pressure has little effect on the variation in spray characteristics and evaporation percentage, nor does the fuel injection velocity shown in Fig. 6. As shown in Ref. 1, the evaporation constant at $T_A = 500$ K will decrease very little with the increase in pressure from 100 to ≈ 300 kPa. The increase in pressure will lead to a higher air density and faster acceleration of the droplets in the axial direction, which the droplets travel a certain downstream distance in slightly less time. However, these effects are weak, resulting in only small decreases in the curves shown in Fig. 5. The effect of increasing the fuel injection velocity will affect the initial relative velocity very little, as the air velocity is much higher than the injection velocity. Also, the residence time is primarily determined by the air velocity; thus, the effect of the injection velocity is very weak. Because of the higher relative velocity, the aerodynamic acceleration of the droplets in the axial direc-

tion will be slightly higher, which means less residence time, thus causing a little less evaporation.

As it was obtained in Ref. 1, a larger initial N value means a more uniform initial spray, which means a lower mass fraction of smaller droplets and thus less initial evaporation, as shown in Fig. 7c. As shown in Ref. 1, a larger initial N value will offer less variation in spray characteristics along downstream distance X, as shown in Figs. 7a and 7b. Also, a larger initial SMD value will result in a lower evaporation percentage as expected and less variation in spray characteristics, as shown in Fig. 8. As a whole, the conclusions drawn in Ref. 1 can be extended to the moving spray conditions.

Conclusions

1) Fuel spray characteristics such as the Sauter mean diameter and N always increase (for initial N values smaller than 4) during the movement of a vaporizing spray in a high-temperature cross-flowing airstream.

2) The most important factors influencing the evaporation of the spray and the variation of the spray characteristics along the downstream distance are: air temperature, air velocity, and initial spray characteristics.

3) A numerical method and a comprehensive computer program have been presented for the calculation of fuel spray characteristics and evaporation in afterburners or ramjet engines.

References

[1]Chin, J. S., Durrett, R., and Lefebvre, A. H., "The Interdependence of Spray Characteristics and Evaporation History of Fuel Spray," *Transactions of ASME, Journal of Engineering for Gas Turbine and Power*, Vol. 106, July 1984, p. 639.

[2]Ranz, W. E. and Marshall, W. R., *"Journal of Chemical Engineering Progress,* Vol. 48, No. 3/4, 1952.

[3]Faeth, G. M. "Current Status of Droplet and Liquid Combustion," *Progress in Energy and Combustion Science,* Vol. 3, No. 4, 1977.

[4]Chin, J. S. and Lefebvre, A. H., "Steady-State Evaporation Characteristics of Hydrocarbon Fuel Drops," *AIAA Journal*, Vol. 21, Oct. 1983, p. 1437.

[5]Spalding, D. B., "The Combustion of Liquid Fuel," *Fourth Symposium (International) on Combustion,* Williams and Wilkins, Baltimore, MD, 1953, p. 847.

[6]Chin, J. S., "The Analysis of Evaporation of Hydrocarbon Fuel Droplet," *Internal Combustion Engine Engineering,* No. 1, 1985 (in Chinese).

[7]Sparrow, E. M., and Gregg, J. L. "The Variable Fluid-Property Problem in Free Convection," *Transactions of the ASME*, Vol. 80, 1958, pp. 879-886.

From the AIAA Progress in Astronautics and Aeronautics Series...

ORBIT-RAISING AND MANEUVERING PROPULSION: RESEARCH STATUS AND NEEDS—v. 89

Edited by Leonard H. Caveny, Air Force Office of Scientific Research

Advanced primary propulsion for orbit transfer periodically receives attention, but invariably the propulsion systems chosen have been adaptations or extensions of conventional liquid- and solid-rocket technology. The dominant consideration in previous years was that the missions could be performed using conventional chemical propulsion. Consequently, major initiatives to provide technology and to overcome specific barriers were not pursued. The advent of reusable launch vehicle capability for low Earth orbit now creates new opportunities for advanced propulsion for interorbit transfer. For example, 75% of the mass delivered to low Earth orbit may be the chemical propulsion system required to raise the other 25% (i.e., the active payload) to geosynchronous Earth orbit; nonconventional propulsion offers the promise of reversing this ratio of propulsion to payload masses.

The scope of the chapters and the focus of the papers presented in this volume were developed in two workshops held in Orlando, Fla., during January 1982. In putting together the individual papers and chapters, one of the first obligations was to establish which concepts are of interest for the 1995-2000 time frame. This naturally leads to analyses of systems and devices. This open and effective advocacy is part of the recently revitalized national forum to clarify the issues and approaches which relate to major advances in space propulsion.

Published in 1984, 569 pp., 6×9, illus., $45.00 Mem., $72.00 List

TO ORDER WRITE: Publications Order Dept., AIAA, 1633 Broadway, New York, N.Y. 10019